ACS OMEGA

http://pubs.acs.org/journal/acsodf

Article

Polarization-Type Potential-Induced Degradation in Front-Emitter p-Type and n-Type Crystalline Silicon Solar Cells

Seira Yamaguchi,*,⊥ Sachiko Jonai,⊥ Kyotaro Nakamura, Kazuhiro Marumoto,* Yoshio Ohshita, and Atsushi Masuda*

Cite This: *ACS Omega* 2022, 7, 36277−36285

Read Online

ACCESS | Metrics & More | Article Recommendations | Supporting Information

ABSTRACT: For SiO_2 layers underneath the SiN_x antireflection/passivation layers of front-emitter p-type c-Si solar cells, this paper presents an investigation into their effects on polarization-type potential-induced degradation (PID), in addition to a comparison of polarization-type PID behavior in front-emitter p-type c-Si cells and front-emitter n-type c-Si cells. After PID tests with a bias of +1000 V, p-type c-Si cells without SiO_2 layers underneath the SiN_x layers showed no degradation, although p-type c-Si cells with approx. 10 nm thick SiO_2 layers showed polarization-type PID, which is characterized by a reduction of the short-circuit current density and the open-circuit voltage. This result implies that highly insulating layers such as SiO_2 layers play an important role in the occurrence of polarization-type PID. Comparison of polarization-type PID in p-type and n-type c-Si cells with SiO_2 layers indicated that degradation in the n-type cells is greater and saturates in a shorter time than in the p-type cells. This result is consistent with an earlier proposed model based on the assumption that polarization-type PID is caused by charge accumulation at K centers in SiN_x layers. The findings described herein are crucially important for elucidating polarization-type PID and verifying the degradation model.

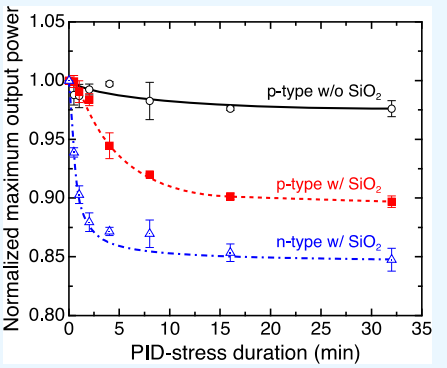

1. INTRODUCTION

Recently, potential-induced degradation (PID) has been identified as a central reliability issue of photovoltaic (PV) cell modules.[1−8] Causing marked degradation in a short time, such as several months, PID is triggered by potential differences between grounded frames and the active circuit of cells in modules in the field. The PID behavior varies to a considerable degree depending on PV cell material, structure, and PID-stress intensity.[7,8] For instance, sodium-penetration-type PID (including shunting-type PID),[1−9] polarization-type PID,[9−22] and corrosion-type PID[19,23−27] are known to occur depending on these factors.

Particularly, polarization-type PID is regarded as the fastest degradation mode among all PID modes.[8] It has been observed for crystalline silicon (c-Si) cells of several types including n-type passivated emitter and rear totally diffused (PERT) cells[9−19] and n-type interdigitated back-contact cells with a front-surface field[20,21] or a front floating emitter.[22] Polarization-type PID is characterized by reduction of the short-circuit current density, J_{SC}, and reduction of the open-circuit voltage, V_{OC}. Polarization-type PID starts to occur within the first few seconds in an accelerated PID test in which a bias of −1000 V is applied at 85 °C.[11,12] Additionally, it occurs even when the applied voltage in the PID test is extremely low, e.g., −50 V.[10] This finding indicates that such PID can occur in small-scale PV systems with low system voltages, such as rooftop PV systems.

As its mechanism, positive (or negative) charge accumulation in the front SiN_x layers of solar cells might cause polarization-type PID.[20] The accumulated charges attract minority carriers and enhance interface recombination via interface defects, leading to reduced J_{SC} and V_{OC}.[20] Charged K centers in SiN_x have been proposed to date as charge sources causing polarization-type PID.[11,12] Based on those mechanisms, conventional p-type c-Si solar cells such as aluminum back surface fields (Al-BSFs) and passivated emitter and rear cells (PERCs) are expected to suffer polarization-type PID under a positive bias. This is because K centers in SiN_x can also be negatively charged under a positive bias and enhance the surface recombination of minority carriers in the n-type emitters. However, few reports have described polarization-type PID at the front side of such conventional p-type c-Si cells.[28] (Note that there are some reports on polarization-type PID at the rear of PERCs under a negative bias.[16,29] On the other hand, this study deals with polarization-type PID at the front side, which is distinguished from the rear-side degradation.) This lack of results from experimentation is

Received: June 21, 2022
Accepted: September 26, 2022
Published: October 7, 2022

probably attributable to the fact that apparent polarization-type PID does not occur in front-emitter p-type c-Si cells. This lack of occurrence might be partly attributable to the fact that polarization-type PID in front-emitter p-type c-Si cells occurs under opposite bias to that causing shunting-type PID,[1−7] which has been studied most actively. Jonai et al. have briefly reported that polarization-type PID occurs under a positive bias in p-type Al-BSF cells with SiN_x/SiO_2 stacked passivation layers[28] and that SiO_2 layers underneath SiN_x layers play an important role in the occurrence of polarization-type PID. Additionally, although a brief comparison of the degradation behaviors of p-type and n-type c-Si cells has been made, no sufficiently detailed comparison has been reported.

This report describes polarization-type PID occurring in front-emitter p-type c-Si cells and discusses effects of SiO_2 layers underneath SiN_x layers on polarization-type PID with more detail than presented earlier.[28] The discussion shows that front-emitter p-type c-Si cells with SiN_x/SiO_2 stacked passivation layers exhibit polarization-type PID, supporting a fair comparison of p-type and n-type cell degradation behaviors by the use of such cells. Subsequently, we made a detailed comparison between polarization-type PID behaviors of the p-type c-Si cells and that of n-type c-Si cells, demonstrating that differences exist in the degradation rate and magnitude. These findings are crucially important for elucidating polarization-type PID and verifying the model proposed previously.

2. EXPERIMENT PROCEDURES

2.1. Solar Cells and Modules. We prepared front-emitter c-Si solar cells of the kinds shown in Figure 1: p-type Al-BSF cells with SiN_x passivation layers, p-type Al-BSF cells with SiN_x/SiO_2 stacked passivation layers, and n-type PERT cells with SiN_x/SiO_2 stacked passivation layers. Their emitter sheet resistances were approximately 60 Ω/□ regardless of the cell type. The SiO_2 layers improve the passivation quality by reducing the interface defect density[30] and are frequently used as passivation layers in n-type PERT cells. The cells without thermally grown SiO_2 layers probably had native oxides. However, such SiO_2 layers are very thin and could not affect the degradation behavior significantly. Therefore, we disregarded the effect of native oxide on the degradation behavior of the cells. These Al-BSF cells and PERT cells were, respectively, those of front-emitter p-type and n-type cells. The solar cells were made of 156 mm × 156 mm pseudo-square wafers. The SiN_x layer and SiO_2 layer thicknesses were, respectively, approximately 80 nm and approximately 10 nm. These thicknesses were applied to both the p-type and n-type cells. The SiN_x layers were deposited using plasma-enhanced chemical vapor deposition (PECVD). The SiO_2 layers were grown by thermal oxidation.

Full-size cells were cleaved into small cell pieces of 20 mm × 20 mm. Standard interconnector ribbons were soldered onto the busbars on both sides of the cells. After soldering, we prepared stacks composed of conventional cover glass/ethylene−vinyl acetate copolymer (EVA) sheet/cell/EVA sheet/typical white backsheet. Mini modules were prepared by laminating the stacks in a module laminator. The lamination process consisted of a degassing step for 5 min and an adhesion step for 15 min. During both steps, the stacks were placed on a stage maintained at 135 °C.

2.2. PID Tests and Characterizations. Accelerated PID tests on the fabricated PV modules were performed by application of a bias of +1000 V for the p-type cells and −1000 V for the n-type cells to connected interconnector ribbons with respect to a grounded aluminum plate placed on the cover glass via an electrically conductive rubber sheet in a chamber maintained at 85 °C. Three identical samples were used for each PID test condition. During the PID tests, the chamber humidity was not controlled. However, the relative humidity in a similar setup was very low (<2%).[31] Consequently, the influence of moisture ingress was disregarded in this study.

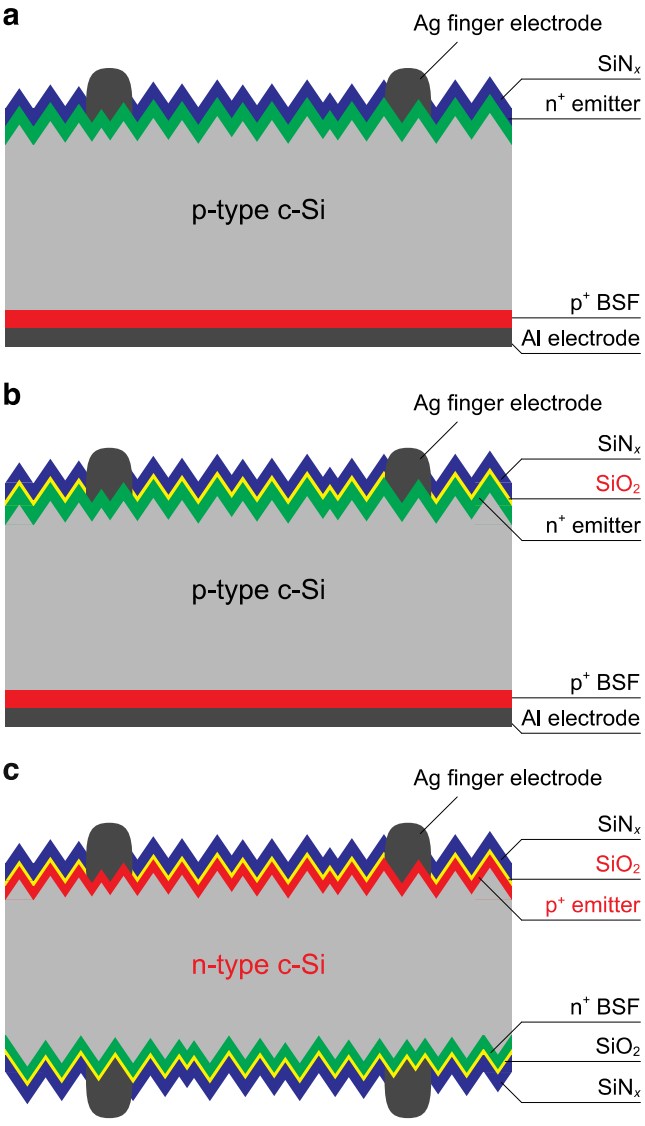

Figure 1. Schematic diagrams of cross sections of the PV cells used for this study: (a) p-type c-Si cells with single-layered SiN_x passivation films, (b) p-type c-Si cells with double-layered SiN_x/SiO_2 passivation films, and (c) n-type c-Si cells with double-layered SiN_x/SiO_2 passivation films.

To evaluate cell degradation, current density−voltage ($J-V$) measurements under one sun illumination and in the dark were taken before and after the PID tests. The J_{SC}, the V_{OC}, the fill factor (FF), and the maximum output power (P_{max}) were acquired from the one sun illuminated $J-V$ curves. From the dark $J-V$ curves, the saturation current density of the first diode (J_{01}) was derived by fitting the curves to a two-diode model.[32] In this two-diode fitting, the ideality factor of the first diode was fixed at 1. External quantum efficiency (EQE)

https://doi.org/10.1021/acsomega.2c03866
ACS Omega 2022, 7, 36277−36285

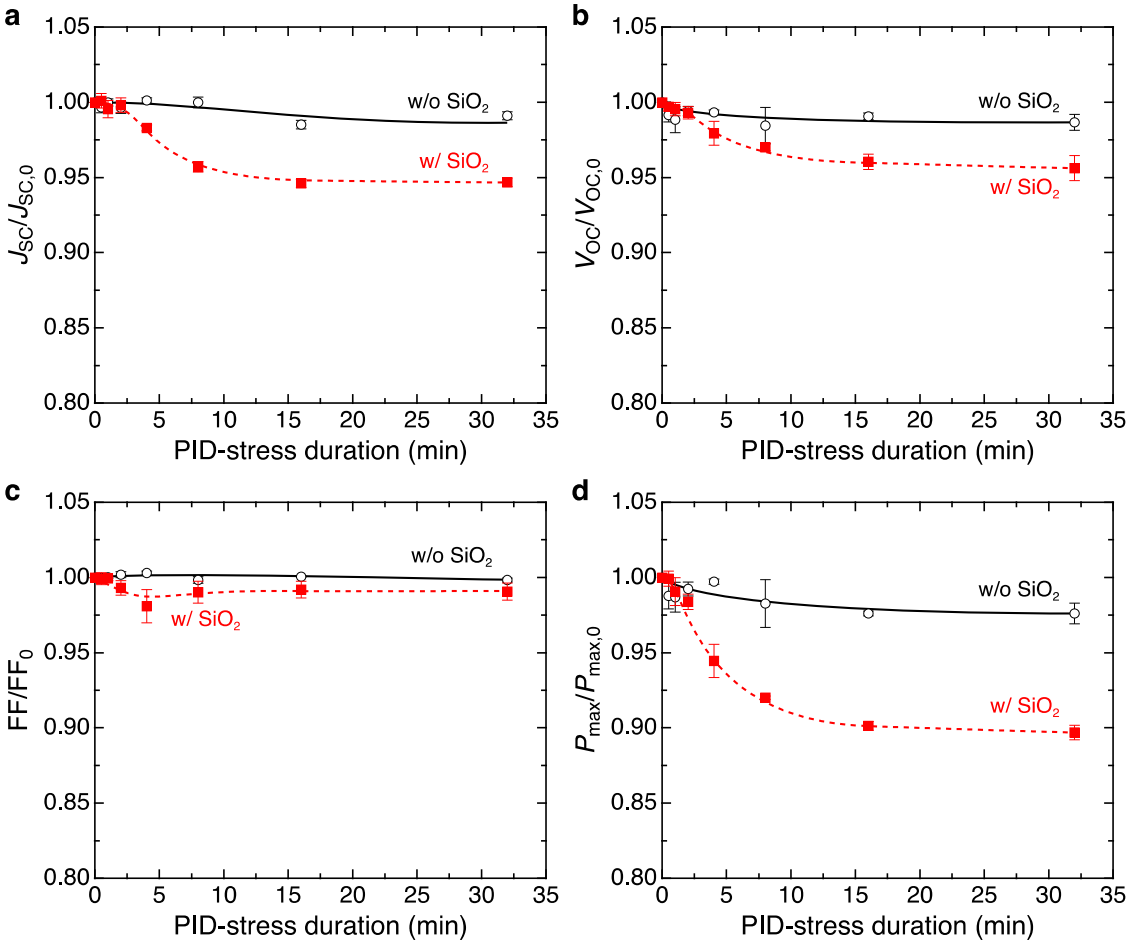

Figure 2. Changes in (a) $J_{SC}/J_{SC,0}$, (b) $V_{OC}/V_{OC,0}$, (c) FF/FF_0, and (d) $P_{max}/P_{max,0}$ of the modules fabricated from the p-type c-Si cells with the SiN_x single-layered passivation films and with the SiN_x/SiO_2 double-layered passivation films undergoing PID tests, for which a bias of +1000 V was applied. Data points show mean values for three identical modules. The error bars correspond to the standard deviation of the mean. Solid and broken lines are guides to the eye.

measurements were also taken before and after the PID tests. All measurements were conducted at 25 °C.

3. RESULTS

This study specifically examined the behaviors of polarization-type PID in conventional front-emitter p-type and n-type c-Si cells. First, we clarified the polarization-type PID behaviors of the Al-BSF c-Si cells under a positive bias and elucidated the effects of SiO_2 layers underneath SiN_x layers on the polarization-type PID. Subsequently, we compared the behaviors of polarization-type PID in p-type Al-BSF c-Si cells and n-type PERT cells.

3.1. Polarization-Type PID in p-Type Cells and Effects of SiO_2 Layers. We first performed the PID tests in which a bias of +1000 V was applied on p-type Al-BSF cells without (Figure 1a) and with (Figure 1b) the SiO_2 layers underneath the SiN_x layers. Figure 2 shows the dependence of $J_{SC}/J_{SC,0}$, $V_{OC}/V_{OC,0}$, FF/FF_0, and $P_{max}/P_{max,0}$ on the PID-stress duration, where subscript 0 denotes the initial values. The p-type cells without the SiO_2 layers exhibit only tiny reductions in the J_{SC} and V_{OC}. The p-type cells with the SiO_2 layers show apparent degradation, as characterized by marked reductions in J_{SC} and V_{OC}. Additionally, the degradation is rapid and tends to saturate within the short time of 16 min. This result implies that the SiO_2 layers underneath the SiN_x layers play an important role in polarization-type PID. The degraded cells recovered their performance losses by application of a negative bias; however, the FF was adversely affected by the recovery treatment (see Figure S1 in the Supporting Information).

Figure 3 shows the J_{01} values of the p-type cells without and with the SiO_2 layers as a function of the PID-stress duration. The initial J_{01} values are high. These high values might be attributable to enhanced edge recombination because of unpassivated edges, which were formed by the cleaving process. The J_{01} of the p-type cells without the SiO_2 layers is almost unchanged before and after the PID tests. However, the J_{01} of the p-type cells with the SiO_2 layers increases considerably after the PID stress. Additionally, the J_{01} of the p-type cells with the SiO_2 layers shows similar saturation behavior to the degradation in the J_{SC} and V_{OC}. This finding indicates that reductions in the J_{SC} and the V_{OC} are caused by enhancement in the interface and/or bulk recombination.

Figure 4a shows the EQE in a short wavelength range of the p-type cells without and with the SiO_2 layers. Figure 4b shows the EQEs at 390 nm of both cells as a function of the PID-stress duration. A difference is evident in the initial EQE, which is probably attributable to an optical loss because of the insertion of the SiO_2 layers. The p-type cells without the SiO_2 layers show almost no reduction in the EQE because of the PID stress. However, the EQE of the cells with SiO_2 is

https://doi.org/10.1021/acsomega.2c03866
ACS Omega 2022, 7, 36277−36285

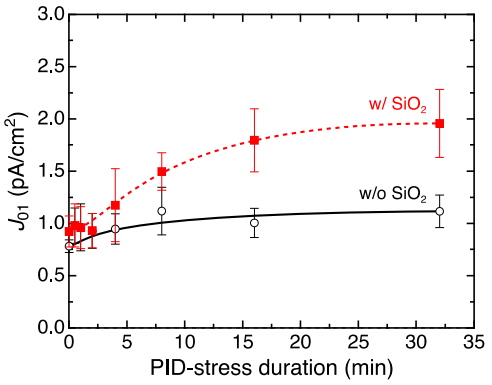

Figure 3. Changes in the J_{01} of the modules fabricated from the p-type c-Si cells with SiN_x single-layered passivation films and with SiN_x/SiO_2 double-layered passivation films undergoing the PID tests, for which a bias of +1000 V was applied. Data points show the mean values for three identical modules. Error bars correspond to the standard deviation of the mean. Solid and broken lines are guides to the eye.

markedly lower in the range of approximately 300−600 nm, concomitantly with increasing PID-stress duration. The reduction ceases within 16 min, similarly to the J_{SC} and V_{OC} reductions in Figure 2. These results indicate that the increase in J_{01} and therefore the reductions in J_{SC} and V_{OC} originate from an interface recombination enhancement at the interface between the n^+ emitters and the passivation layers.

3.2. Comparison of Degradation Behaviors of p-Type and n-Type Solar Cells. Here, we compare the degradation behaviors of the p-type Al-BSF cells with SiO_2 (Figure 1b) with those of the n-type PERT cells with SiO_2 (Figure 1c). It is noteworthy that the p-type Al-BSF cells were subjected to PID tests with a bias of +1000 V, whereas the n-type PERT cells were subjected to PID tests with a bias of −1000 V. This finding indicates that negative and positive charges are injected, respectively, to SiN_x of the p-type cells and n-type cells during the PID tests. Figure 5 presents the $J_{SC}/J_{SC,0}$, $V_{OC}/V_{OC,0}$, FF/FF_0, and $P_{max}/P_{max,0}$ of the p-type Al-BSF cells and the n-type PERT cells as a function of the PID-stress duration. Data of the p-type cells are the same as those labeled as "w/ SiO_2" in Figure 2. Two main differences exist between the degradation behaviors of the p-type cells and the n-type cells found in Figure 5. One is in the time necessary for the degradation's saturation. Degradation of the p-type cells saturates within 16 min. Degradation of the n-type cells saturates almost completely within 8 min. The other is in the degradation magnitude. After saturation, the degradation in the n-type cells is twice that in the p-type cells. These results indicate that polarization-type PID in n-type PERT cells is greater and tends to saturate within a shorter time than that in p-type Al-BSF cells.

Figure 6 shows the J_{01}'s of the p-type cells and n-type cells as a function of the PID-stress duration. The J_{01} values of both cells increase rapidly and saturate within a short time. However, the increase in J_{01} of the n-type cells is greater and leads to more rapid saturation than that for the p-type cells. This trend is consistent with the J_{SC} and V_{OC} degradation behavior shown in Figure 5.

Figure 7a shows an EQE reduction in a short wavelength range of the n-type cells caused by PID stress. The EQE of the n-type cells reduces rapidly in the range of approximately 300−600 nm. The reduction is almost complete within 8 min. As shown in Figure 7b, the EQE at 390 nm of the n-type cells decreases considerably. The reduction stops within a shorter time than that of the p-type cells, which is a similar trend to the J_{SC} and V_{OC} reduction displayed in Figure 5.

4. DISCUSSION

4.1. Effects of SiO_2 Layers on Polarization-Type PID in p-Type Cells. Based on the proposed mechanisms,[11,12] conventional front-emitter p-type c-Si solar cells are expected to undergo polarization-type PID under a positive bias. However, few reports have described polarization-type PID in such p-type c-Si cells.[28] One earlier brief report[28] explained that polarization-type PID occurs under a positive bias in p-type Al-BSF cells with SiN_x/SiO_2 stacked passivation layers and that SiO_2 layers underlying the SiN_x layers play an important role in the occurrence of polarization-type PID. Herein, we further discuss the polarization-type PID in conventional p-type c-Si cells and the effects of SiO_2 layers on the occurrence of polarization-type PID based on the proposed degradation mechanism.[11,12]

Figure 2 shows that the p-type cells exhibit apparent degradation under a positive bias only when having SiO_2 layers underneath the SiN_x layers. The degradation occurred rapidly and saturated in a short time. Additionally, the modules showed recovery under negative bias, which was the opposite bias used for the PID tests. The observed degradation was characterized by reductions in the J_{SC} and V_{OC}. As Figures 3

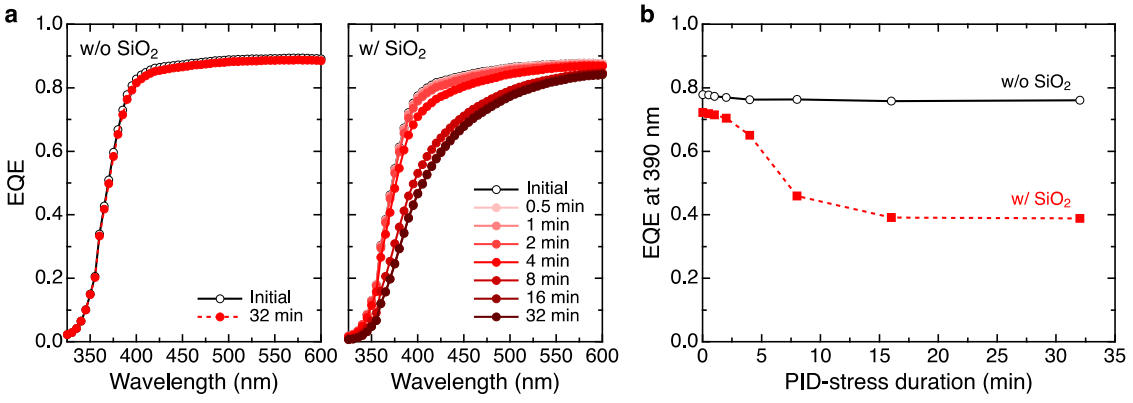

Figure 4. (a) PID-stress duration dependence of the EQEs in a short wavelength range of the modules fabricated from the p-type c-Si cells without and with SiO_2 passivation films. (b) Changes in the EQEs of both modules at 390 nm wavelength. Solid and broken lines are guides to the eye.

https://doi.org/10.1021/acsomega.2c03866
ACS Omega 2022, 7, 36277−36285

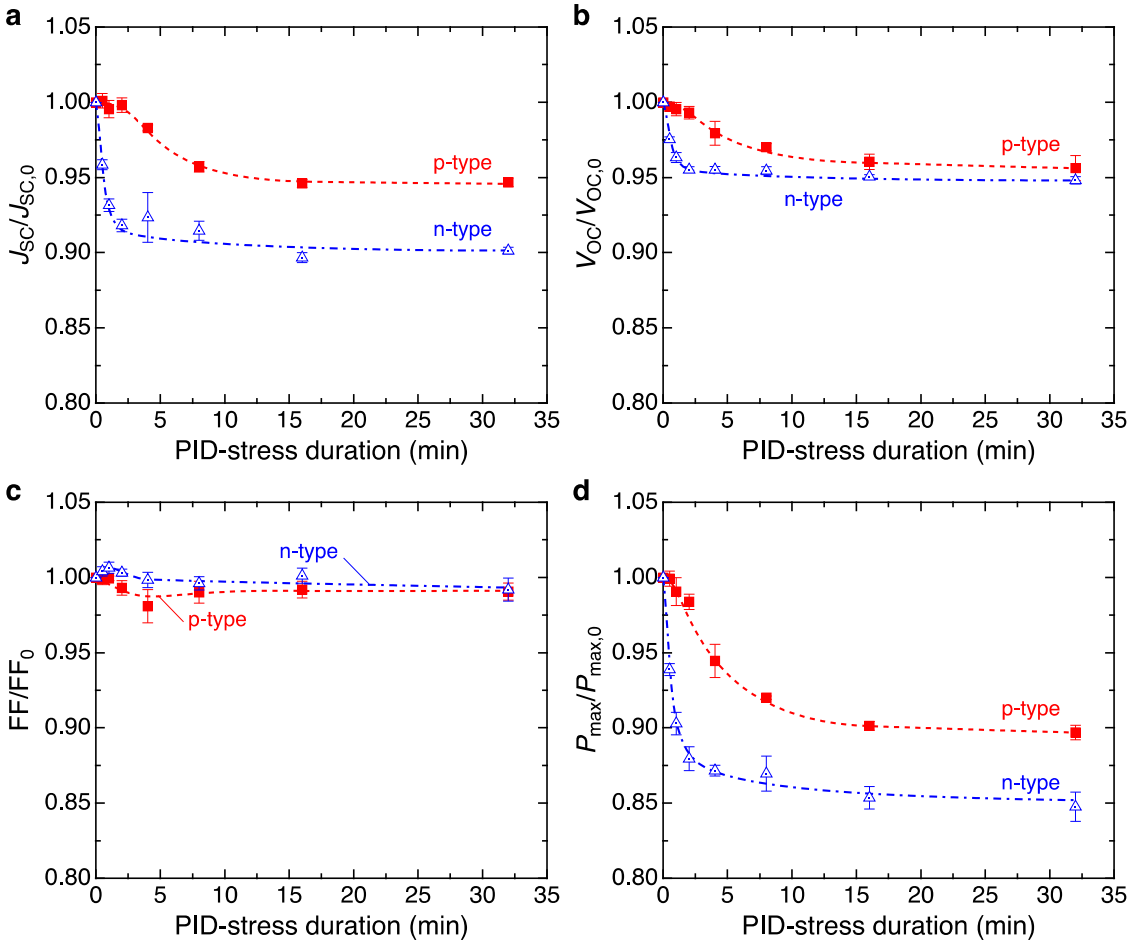

Figure 5. Dependence of (a) $J_{SC}/J_{SC,0}$, (b) $V_{OC}/V_{OC,0}$, (c) FF/FF$_0$, and (d) $P_{max}/P_{max,0}$ of the modules fabricated from the p-type and n-type c-Si cells with the SiN_x/SiO_2 double-layered passivation films on the PID-stress duration. The p-type cell modules were subjected to the PID tests with a bias of +1000 V, whereas the n-type ones were subjected to the PID tests with a bias of −1000 V. Data labeled as "p-type" were extracted from Figure 2. Data points show mean values for three identical modules. The error bars correspond to the standard deviation of the mean. Broken and chain lines are guides to the eye.

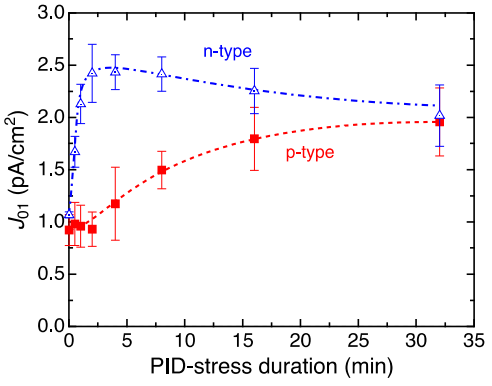

Figure 6. Changes in the J_{01}'s of the modules fabricated from the p-type and n-type c-Si cells with the SiN_x/SiO_2 double-layered passivation films in the PID tests. The p-type cell modules underwent PID tests with a bias of +1000 V, whereas the n-type cell modules underwent the PID tests with a bias of −1000 V. Data labeled as "p-type" were extracted from Figure 3. Data points represent mean values for three identical modules. Error bars correspond to the standard deviation of the mean. Broken and chain lines are guides to the eye.

and 4 show, the reductions in J_{SC} and V_{OC} were accompanied by an increase in J_{01} and a decrease in EQE at short wavelengths, indicating that the degradation was attributable to enhanced interface recombination at the passivation layer/emitter interfaces. These features correspond to those of polarization-type PID reported previously.[11,12] Therefore, the degradation was fundamentally identical to polarization-type PID that has been observed frequently in n-type c-Si solar cells to date. This discussion suggests that conventional p-type c-Si cells undergo polarization-type PID when having thin SiO_2 layers underneath the SiN_x passivation and antireflection layers.

Based on the "K-center model" proposed earlier in the literature,[11,12] we can consider why the SiO_2 layers cause polarization-type PID in p-type c-Si cells. Figure 8 presents the schematic diagrams of charge accumulation and dissipation processes in p-type c-Si cells without and with SiO_2 layers. By application of a positive bias, negative charges reach the SiN_x surface (Figure 8a-1 and b-1). These negative charges extract holes from neutral K centers (K^0 centers) and positively charged K centers (K^+ centers) in the SiN_x layer, where the K centers are dangling bonds backbonded to three nitrogen atoms. Thereby, negatively charged K centers (K^- centers) are left in the SiN_x layer; the net charge of the SiN_x layer is shifted toward negative (Figure 8a-2 and b-2). This negative shift of the net charge causes upward band bending in the surface region of the emitter and reduces the J_{SC} and V_{OC}. If there is

https://doi.org/10.1021/acsomega.2c03866
ACS Omega 2022, 7, 36277−36285

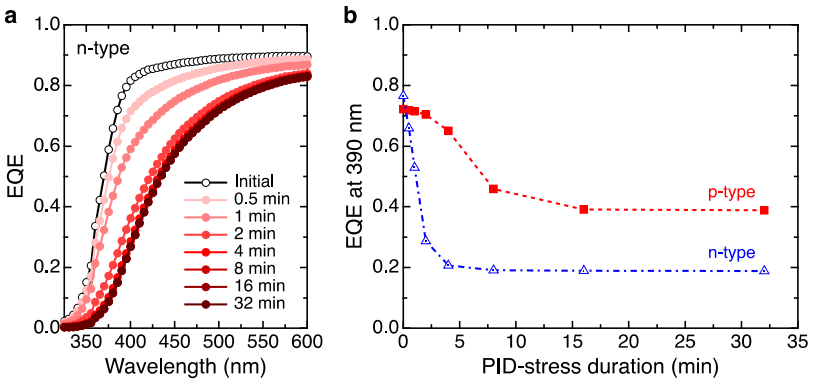

Figure 7. (a) PID-stress duration dependence of the EQEs in a short wavelength range of the modules fabricated from the n-type c-Si cells with the double-layered SiN_x/SiO_2 passivation films. (b) Changes in the EQEs at 390 nm wavelength of modules from p-type and n-type cells with double-layered passivation films. Data labeled as "p-type" were extracted from Figure 4b. Broken and chain lines are guides to the eye.

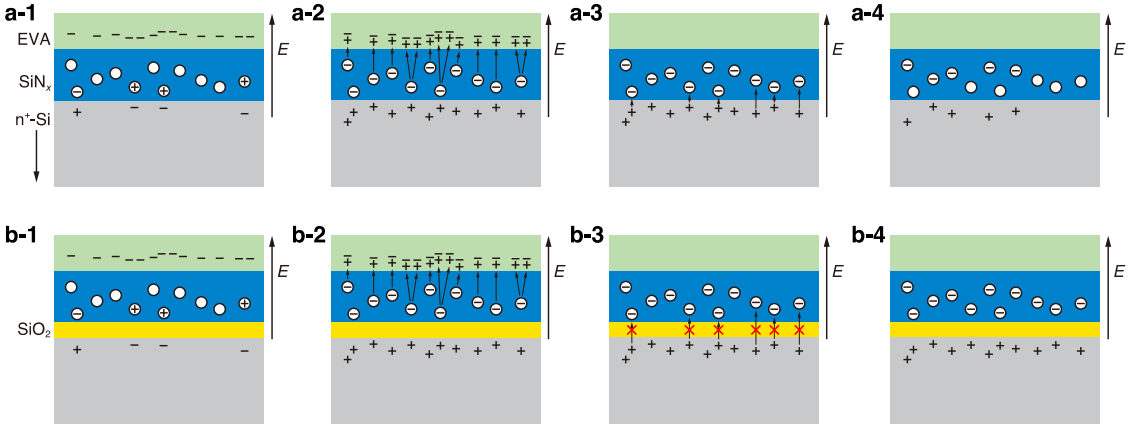

Figure 8. Schematic diagrams of effects of the SiO_2 layers underneath the SiN_x layers: degradation processes in p-type cells (a) without SiO_2 and (b) with SiO_2. Circles, "+" symbols, and "−" symbols in this figure respectively represent K centers, positive charges, and negative charges. The red × symbols in panel (b-3) indicate that carrier transport across the SiO_2 layer does not occur. This figure presents the cross-sectional diagrams near the emitter surfaces of the p-type cells. Therefore, n^+-Si emitter layers are portrayed in these figures.

no SiO_2 layer underneath the SiN_x layer, then negative charges accumulated in the SiN_x layer are regarded as dissipated by charge transport between the SiN_x layer and the n^+ emitter. Then, no apparent degradation is observed (Figure 8a-3 and a-4). However, if the cell has a SiO_2 layer, then the charge transport between the SiN_x layer and the n^+ emitter is prevented. Most of the negative charges remain (Figure 8b-3 and b-4). These remaining negative charges attract minority carriers, holes, to the passivation/emitter interface. Thereby, interface recombination is enhanced. (In other words, the upward band bending that enhances interface recombination of minority carriers is maintained.)

Apart from the mechanistic aspect, one can discuss the effects of the application of SiO_2 in practical terms. Several groups have proposed that SiO_2 layers underneath the SiN_x layers prevent shunting-type PID.[33,34] Therefore, such SiO_2 layers might be used as preventive measures against the shunting-type PID that is known to occur under a negative bias. However, the application of SiO_2 layers might lead to some unfavorable outcomes. As discussed above, one is that such SiO_2 layers might cause polarization-type PID. Actually, p-type cells with SiO_2 layers are resistant to shunting-type PID. However, cells near the positive end of the string show polarization-type PID because of the SiO_2 layers. Another unfavorable outcome is related to the recovery of the shunting-type PID by a positive bias. The shunting-type PID is reportedly recovered by application of a positive bias.[2,3] If this recovery treatment is applied to p-type c-Si cells with SiO_2 layers, then the shunting-type PID can be recovered effectively, but polarization-type PID occurs instead. Figure 9 presents an example, showing the one sun illuminated $J-V$ curves of a p-type c-Si cell with a SiO_2 layer underneath the SiN_x layer

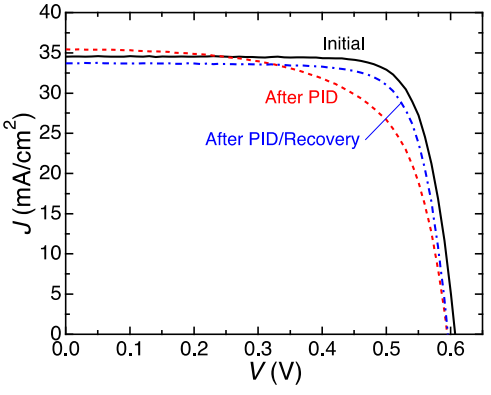

Figure 9. One sun illuminated $J-V$ curves of modules fabricated from p-type cells with the double-layered SiN_x/SiO_2 passivation films before and after PID tests with −1000 V for 16 h and after subsequent recovery tests with +1000 V for 16 h.

https://doi.org/10.1021/acsomega.2c03866
ACS Omega 2022, 7, 36277−36285

before and after a PID test with −1000 V at 85 °C for 16 h and after recovery treatment with +1000 V at 85 °C for 16 h. After the PID test, the p-type c-Si cell shows shunting-type PID, which is caused mainly by a reduction in the FF. After the recovery treatment, the FF reduction is recovered. However, the J_{SC} and V_{OC} are reduced instead. In addition to these, an additional process must be applied to fabricate SiO_2 layers. For these reasons, other means such as the use of high-refractive-index SiN_x layers[35] are more favorable as preventive measures against shunting-type PID.

4.2. Origins of Differences in Degradation Behaviors of p-Type and n-Type Solar Cells. As described above, p-type c-Si cells were found to undergo polarization-type PID when SiO_2 layers are situated underneath the SiN_x layers. This finding enables a fair comparison between the polarization-type PID behavior of p-type c-Si cells and the behavior of n-type c-Si cells. For this study, we used Al-BSF cells and n-type PERT cells, respectively, as p-type and n-type c-Si cells. Fundamentally, findings in this study are applicable to cells of other types that have similar front-surface structures. For example, p-type PERCs have almost the same front-side structure as the Al-BSF cells. Therefore, the findings obtained for the p-type cells in this study are applicable to polarization-type PID in p-type PERCs and other cells with a similar front-surface structure.

Results show that polarization-type PID in the n-type c-Si cells saturated more rapidly and that the saturation was greater than that in the p-type cells (Figure 5). As in J_{SC} and V_{OC} degradation, the J_{01} and EQE of the n-type cells degraded more rapidly and to a greater degree than those of the p-type cells (Figures 6 and 7). First, one can consider why the polarization-type PID in the n-type c-Si cells saturates more rapidly.

Figure 10 portrays a schematic diagram explaining why the times necessary for the saturation of polarization-type PID

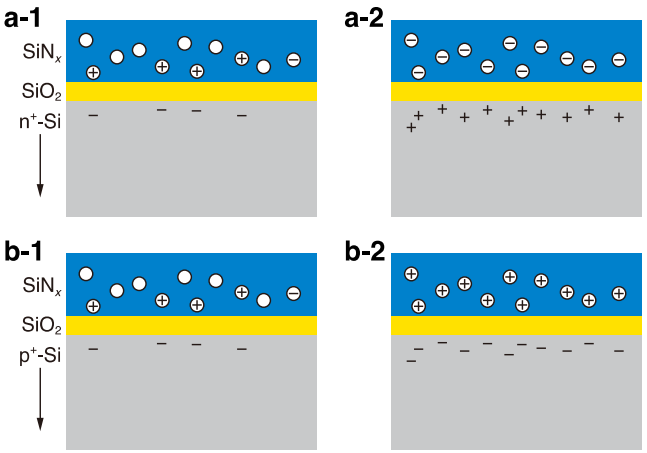

Figure 10. Schematic diagrams of charge accumulation processes before and after saturation for (a) p-type and (b) n-type c-Si cells. The circles, the "+" symbols, and the "−" symbols in this figure respectively represent K centers, positive charges, and negative charges. This figure illustrates the cross-sectional diagrams near the emitter surfaces of the cells. Therefore n^+-Si emitter layers and p^+-Si emitter layers appear respectively for p-type and n-type cells.

differ in p-type and n-type c-Si cells. Based on the proposed model,[11,12] the saturation of degradation can be explained as the saturation of the density of K^- or K^+ centers. The p-type cells are degraded under a positive bias. The saturation of their polarization-type PID corresponds to saturation of the K^- center density (Figure 10a). However, the saturation of the polarization-type PID of the n-type cells is attributable to saturation of the K^+ center density (Figure 10b). Generally, SiN_x layers on c-Si substrates tend to be positively charged.[36] Therefore, the SiN_x layers in both cells are slightly positively charged (Figure 10a-1 and b-1). For p-type cells, positively charged SiN_x layers are expected to be completely negatively charged to achieve saturation of degradation. However, for the n-type cells, the saturation of degradation is achieved by further positively charging SiN_x layers that were originally positively charged to a certain degree. For this reason, degradation in the n-type cells can saturate by supplying fewer charges, which explains the difference in the saturation times.

Based on the results of our earlier study,[12] we estimated the difference in the times required for p-type and n-type cells' polarization-type PID to saturate. For that study,[12] we used SiN_x layers similarly fabricated in the PECVD apparatus, the same as used in the present study. Therefore, the K-center densities measured in the respective studies are regarded as similar. In the earlier study,[12] the positive charge density was approximately $2 \times 10^{12}/cm^2$ before PID tests. After PID tests, the positive charge density saturated to approximately $7 \times 10^{12}/cm^2$. In this case, the positive charge density that should be supplied on the SiN_x in the n-type cells for polarization-type PID to saturate is therefore just approximately $5 \times 10^{12}/cm^2$. For p-type cells, the necessary negative charge density is approximately $9 \times 10^{12}/cm^2$, which is markedly higher than the necessary positive charge density for n-type cells. This result is consistent with the fact that the time necessary for saturation of the degradation in the n-type cells was half that in the p-type cells. This result showing consistency also verifies our K-center model.

The reasons behind the difference in the magnitude of the degradation remain unclear. The magnitude of polarization-type PID depends on many factors, such as the quality of chemical passivation, the junction depth, and the emitter-surface doping concentration. However, the same SiO_2 layers were used in the p-type and n-type cells in this study, and the interface recombination velocities are considered not to be significantly different. One possible candidate is the emitter-surface doping concentration. The B emitters of our n-type cells experienced a B-rich-layer removal process, which might result in low emitter-surface doping concentrations. Also, the low solubility of B in Si may contribute to the low emitter-surface doping concentrations. Such a low emitter-surface doping concentration is sensitive to changes in the fixed charge density. Therefore, it is also sensitive to polarization-type PID.[17] This hypothesis is not inconsistent with the results obtained from our experiments. However, we have not identified the actual reasons for the difference in the magnitude of the degradation. Much additional work is necessary for complete understanding.

5. CONCLUSIONS

This study investigated the effects of SiO_2 layers underneath the SiN_x layers of conventional p-type c-Si cells on their polarization-type PID. In addition, a comparison of the behaviors of polarization-type PID in p-type c-Si cells and n-type c-Si cells was made.

Results show that, under a positive bias, p-type c-Si cells show apparent degradation characterized by reductions in J_{SC} and V_{OC} when having SiO_2 layers underneath the SiN_x layers.

https://doi.org/10.1021/acsomega.2c03866
ACS Omega 2022, 7, 36277−36285

We also found that degradation occurs rapidly and saturates within a short time. Additionally, dark $J-V$ and EQE measurements revealed that the degradation is caused by enhancement of interface recombination at the passivation layer/emitter interface. From these results, the degradation was identified as polarization-type PID. Based on the "K-center model", such SiO_2 layers prevent charge transport between the emitters and the SiN_x layers and maintain accumulated charges in the SiN_x layers. Thereby, stable polarization-type PID occurs.

By comparison of polarization-type PID in the p-type and n-type c-Si cells with SiO_2 layers, we found that n-type cell degradation is greater and that it saturates in a shorter time than in the p-type cells. This difference in the saturation time is explained as follows. The SiN_x layers on c-Si substrates generally tend to be positively charged. The number of positive charges necessary to convert all the K centers into K^+ centers is regarded as less than that of negative charges necessary to convert all of the K centers into K^- centers. This finding is consistent with those of the K-center model. The magnitude of polarization-type PID depends on various factors such as the quality of chemical passivation, the junction depth, and the emitter-surface doping concentration. Much additional work must be undertaken to understand the phenomenon completely.

■ ASSOCIATED CONTENT

Supporting Information

The Supporting Information is available free of charge at https://pubs.acs.org/doi/10.1021/acsomega.2c03866.

Results of recovery tests on degraded p-type and n-type c-Si cell modules (PDF)

■ AUTHOR INFORMATION

Corresponding Authors

Seira Yamaguchi − *Graduate School of Science and Technology, Niigata University, Niigata 950-2181, Japan; Division of Materials Science, Faculty of Pure and Applied Sciences, University of Tsukuba, Tsukuba, Ibaraki 305-8573, Japan;* orcid.org/0000-0002-2761-8308; Email: yamaguchi@ims.tsukuba.ac.jp

Kazuhiro Marumoto − *Division of Materials Science, Faculty of Pure and Applied Sciences, University of Tsukuba, Tsukuba, Ibaraki 305-8573, Japan; Tsukuba Research Center for Energy Materials Science (TREMS), University of Tsukuba, Tsukuba, Ibaraki 305-8571, Japan;* orcid.org/0000-0001-9792-0775; Email: marumoto@ims.tsukuba.ac.jp

Atsushi Masuda − *Graduate School of Science and Technology, Niigata University, Niigata 950-2181, Japan; Interdisciplinary Research Center for Carbon-Neutral Technologies, Niigata University, Niigata 950-2181, Japan;* Email: a-masuda@eng.niigata-u.ac.jp

Authors

Sachiko Jonai − *Graduate School of Science and Technology, Niigata University, Niigata 950-2181, Japan*

Kyotaro Nakamura − *Graduate School of Engineering, Toyota Technological Institute, Nagoya 468-8511, Japan*

Yoshio Ohshita − *Graduate School of Engineering, Toyota Technological Institute, Nagoya 468-8511, Japan*

Complete contact information is available at: https://pubs.acs.org/10.1021/acsomega.2c03866

Author Contributions

⊥S.Y. and S.J. contributed equally to this work.

Notes

The authors declare no competing financial interest.

■ ACKNOWLEDGMENTS

The authors thank Kazuo Muramatsu of NAMICS Corporation, Japan for metallization of the cells. This work was supported by the New Energy and Industrial Technology Development Organization, Japan, the Iketani Science and Technology Foundation, Japan, and the Japan Science and Technology Agency MIRAI (Grant Numbers: JPMJMI20C5, JPMJMI22C1), Japan.

■ REFERENCES

(1) Pingel, S.; Frank, O.; Winkler, M.; Daryan, S.; Geipel, T.; Hoehne, H.; Berghold, J. In *Potential Induced Degradation of Solar Cells and Panels*, Proceedings of the 35th IEEE Photovoltaic Specialists Conference; IEEE: Piscataway, NJ, 2010; pp 2817−2822.

(2) Berghold, J.; Frank, O.; Hoehne, H.; Pingel, S.; Richardson, B.; Winkler, M. In *Potential Induced Degradation of Solar Cells and Panels*, Proceedings of the 25th European Photovoltaic Solar Energy Conference Exhibition/5th World Conference Photovoltaic Energy Conversion; WIP: Munich, Germany, 2010; pp 3753−3759.

(3) Hacke, P.; Kempe, M.; Terwilliger, K.; Glick, S.; Call, N.; Johnston, S.; Kurtz, S.; Bennett, I.; Kloos, M. In *Characterization of Multicrystalline Silicon Modules with System Bias Voltage Applied in Damp Heat*, Proceedings of the 25th European Photovoltaic Solar Energy Conference Exhibition/5th World Conference Photovoltaic Energy Conversion; WIP: Munich, Germany, 2010; pp 3760−3765.

(4) Naumann, V.; Lausch, D.; Graff, A.; Werner, M.; Swatek, S.; Bauer, J.; Hähnel, A.; Breitenstein, O.; Großer, S.; Bagdahn, J.; Hagendorf, C. The role of stacking faults for the formation of shunts during potential-induced degradation of crystalline Si solar cells. *Phys. Status Solidi RRL* **2013**, *7*, 315−318.

(5) Naumann, V.; Lausch, D.; Hähnel, A.; Bauer, J.; Breitenstein, O.; Graff, A.; Werner, M.; Swatek, S.; Großer, S.; Bagdahn, J.; Hagendorf, C. Explanation of potential-induced degradation of the shunting type by Na decoration of stacking faults in Si solar cells. *Sol. Energy Mater. Sol. Cells* **2014**, *120*, 383−389.

(6) Yamaguchi, S.; Masuda, A.; Ohdaira, K. Behavior of the potential-induced degradation of photovoltaic modules fabricated using flat mono-crystalline silicon cells with different surface orientations. *Jpn. J. Appl. Phys.* **2016**, *55*, No. 04ES14.

(7) Luo, W.; Khoo, Y. S.; Hacke, P.; Naumann, V.; Lausch, D.; Harvey, S. P.; Singh, J. P.; Chai, J.; Wang, Y.; Aberle, A. G.; Ramakrishna, S. Potential-induced degradation in photovoltaic modules: a critical review. *Energy Environ. Sci.* **2017**, *10*, 43−68.

(8) Yamaguchi, S.; Van Aken, B. B.; Masuda, A.; Ohdaira, K. Potential-induced degradation in high-efficiency n-type crystalline-silicon photovoltaic modules: A literature review. *Sol. RRL* **2021**, *5*, No. 2100708.

(9) Komatsu, Y.; Yamaguchi, S.; Masuda, A.; Ohdaira, K. Multistage performance deterioration in n-type crystalline silicon photovoltaic modules undergoing potential-induced degradation. *Microelectron. Reliab.* **2018**, *84*, 127−133.

(10) Hara, K.; Jonai, S.; Masuda, A. Potential-induced degradation in photovoltaic modules based on n-type single crystalline Si solar cells. *Sol. Energy Mater. Sol. Cells* **2015**, *140*, 361−365.

(11) Yamaguchi, S.; Masuda, A.; Ohdaira, K. Progression of rapid potential-induced degradation of n-type single-crystalline silicon photovoltaic modules. *Appl. Phys. Express* **2016**, *9*, No. 112301.

(12) Yamaguchi, S.; Nakamura, K.; Masuda, A.; Ohdaira, K. Rapid progression and subsequent saturation of polarization-type potential-

induced degradation of n-type front-emitter crystalline-silicon photovoltaic modules. *Jpn. J. Appl. Phys.* **2018**, *57*, No. 122301.
(13) Suzuki, T.; Yamaguchi, S.; Nakamura, K.; Masuda, A.; Ohdaira, K. Effect of a SiO_2 film on the potential-induced degradation of n-type front-emitter crystalline Si photovoltaic modules. *Jpn. J. Appl. Phys.* **2020**, *59*, No. SCCD02.
(14) Bae, S.; Oh, W.; Lee, K. D.; Kim, S.; Kim, H.; Park, N.; Chan, S.-I.; Park, S.; Kang, Y.; Lee, H.-S.; Kim, D. Potential induced degradation of n-type crystalline silicon solar cells with p^+ front junction. *Energy Sci. Eng.* **2017**, *5*, 30−37.
(15) Luo, W.; Khoo, Y. S.; Singh, J. P.; Wong, J. K. C.; Wang, Y.; Aberle, A. G.; Ramakrishna, S. Investigation of potential-induced degradation in n-PERT bifacial silicon photovoltaic modules with a glass/glass structure. *IEEE J. Photovoltaics* **2018**, *8*, 16−22.
(16) Luo, W.; Hacke, P.; Hsian, S. M.; Wang, Y.; Aberle, A. G.; Ramakrishna, S.; Khoo, Y. S. Investigation of the impact of illumination on the polarization-type potential-induced degradation of crystalline silicon photovoltaic modules. *IEEE J. Photovoltaics* **2018**, *8*, 1168−1173.
(17) Yamaguchi, S.; Van Aken, B. B.; Stodolny, M. K.; Löffler, J.; Masuda, A.; Ohdaira, K. Effects of passivation configuration and emitter surface doping concentration on polarization-type potential-induced degradation in n-type crystalline-silicon photovoltaic modules. *Sol. Energy Mater. Sol. Cells* **2021**, *226*, No. 111074.
(18) Yamaguchi, S.; Nakamura, K.; Semba, T.; Ohdaira, K.; Marumoto, K.; Ohshita, Y.; Masuda, A. Effects of SiN_x refractive index and SiO_2 thickness on polarization-type potential-induced degradation in front-emitter n-type crystalline-silicon photovoltaic cell modules. *Energy Sci. Eng.* **2022**, *10*, 2268−2275.
(19) Ohdaira, K.; Komatsu, Y.; Suzuki, T.; Yamaguchi, S.; Masuda, A. Influence of sodium on the potential-induced degradation for n-type crystalline silicon photovoltaic modules. *Appl. Phys. Express* **2019**, *12*, No. 064004.
(20) Swanson, R.; Cudzinovic, M.; DeCeuster, D.; Desai, V.; Jürgens, J.; Kaminar, N.; Mulligan, W.; Rodrigues-Barbarosa, L.; Rose, D.; Smith, D.; Terao, A.; Wilson, K. In *The Surface Polarization Effect In High-efficiency Silicon Solar Cells*, Tech. Dig. 15th Int. Photovoltaic Sci. Eng. Conf., 2005; pp 410−411.
(21) Ishii, T.; Masuda, A. Annual degradation rates of recent crystalline silicon photovoltaic modules. *Prog. Photovolt: Res. Appl.* **2017**, *25*, 953−967.
(22) Halm, A.; Schneider, A.; Mihailetchi, V. D.; Koduvelikulathu, L. J.; Popescu, L. M.; Galbiati, G.; Chu, H.; Kopecek, R. Potential-induced degradation for encapsulated n-type IBC solar cells with front floating emitter. *Energy Procedia* **2015**, *77*, 356−363.
(23) Sporleder, K.; Naumann, V.; Bauer, J.; Richter, S.; Hähnel, A.; Großer, S.; Turek, M.; Hagendorf, C. Local corrosion of silicon as root cause for potential-induced degradation at the rear side of bifacial PERC solar cells. *Phys. Status Solidi RRL* **2019**, *13*, No. 1900163.
(24) Sporleder, K.; Naumann, V.; Bauer, J.; Richter, S.; Hähnel, A.; Großer, S.; Turek, M.; Hagendorf, C. Microstructural analysis of local silicon corrosion of bifacial solar cells as root cause of potential-induced degradation at the rear side. *Phys. Status Solidi A* **2019**, *216*, No. 1900334.
(25) Sporleder, K.; Naumann, V.; Bauer, J.; Richter, S.; Hähnel, A.; Großer, S.; Turek, M.; Hagendorf, C. Root cause analysis on corrosive potential-induced degradation effects at the rear side of bifacial silicon PERC solar cells. *Sol. Energy Mater. Sol. Cells* **2019**, *201*, No. 110062.
(26) Yamaguchi, S.; Yamamoto, C.; Ohdaira, K.; Masuda, A. Reduction in the short-circuit current density of silicon heterojunction photovoltaic modules subjected to potential-induced degradation tests. *Sol. Energy Mater. Sol. Cells* **2017**, *161*, 439−443.
(27) Yamaguchi, S.; Yamamoto, C.; Ohdaira, K.; Masuda, A. Comprehensive study of potential-induced degradation in silicon heterojunction photovoltaic cell modules. *Prog. Photovolt: Res. Appl.* **2018**, *26*, 697−708.
(28) Jonai, S.; Nakamura, K.; Masuda, A. Universal explanation for degradation by charge accumulation in crystalline Si photovoltaic modules with application of high voltage. *Appl. Phys. Express* **2019**, *12*, No. 101003.
(29) Sporleder, K.; Naumann, V.; Bauer, J.; Hevisov, D.; Turek, M.; Hagendorf, C. Time-resolved investigation of transient field effect passivation states during potential-induced degradation and recovery of bifacial silicon solar cells. *Sol. RRL* **2021**, *5*, No. 2100140.
(30) Zhuang, Y. F.; Zhong, S. H.; Liang, X. J.; Kang, H. J.; Li, Z. P.; Shen, W. Z. Application of SiO_2 passivation technique in mass production of silicon solar cells. *Sol. Energy Mater. Sol. Cells* **2019**, *193*, 379−386.
(31) Yamaguchi, S.; Jonai, S.; Hara, K.; Komaki, H.; Shimizu-Kamikawa, Y.; Shibata, H.; Niki, S.; Kawakami, Y.; Masuda, A. Potential-induced degradation of $Cu(In,Ga)Se_2$ photovoltaic modules. *Jpn. J. Appl. Phys.* **2015**, *54*, No. 08KC13.
(32) Wolf, M.; Noel, G. T.; Stirn, R. J. Investigation of the double exponential in the current−voltage characteristics of silicon solar cells. *IEEE Trans. Electron Devices* **1977**, *24*, 419−428.
(33) Nagel, H.; Saint-Cast, P.; Glatthaar, M.; Glunz, S. W. In *Inline Processes for the Stabilization of P-type Si Solar Cells Against Potential-induced Degradation*, Proceedings of the 29th European Photovoltaic Solar Energy Conference Exhibition; WIP: Munich, Germany, 2014; pp 2351−2355.
(34) Yang, Y.; Zhao, Y. F.; Tang, C. S.; Zou, S.; Yu, Y. Q.; Ma, X. P.; Zhou, Y.; Su, X. D.; Xin, Y. Reducing potential induced degradation of silicon solar cells by using a liquid oxidation technique. *Sol. Energy Mater. Sol. Cells* **2018**, *183*, 101−106.
(35) Nagel, H.; Metz, A.; Wangemann, K. In *Crystalline Si Solar Cells and Modules Featuring Excellent Stability Against Potential-induced Degradation*, Proceedings of the 26th European Photovoltaic Solar Energy Conference Exhibition; WIP: Munich, Germany, 2011; pp 3107−3112.
(36) Hezel, R.; Jaeger, K. Low-temperature surface passivation of silicon for solar cells. *J. Electrochem. Soc.* **1989**, *136*, 518−523.

https://doi.org/10.1021/acsomega.2c03866
ACS Omega 2022, 7, 36277−36285